COO-3151-13

LATTICE VIBRATIONS OF NON-CRYSTALLINE SOLIDS

N. W. Ashcroft, R. B. Stephens, and R. O. Pohl

Department of Physics
Cornell University
Ithaca, New York 14850

September 1972

DISCLAIMER

Lattice Vibrations of Non-crystalline Solids*

N. W. Ashcroft, R. B. Stephens, and R. O. Pohl

Department of Physics
Cornell University
Ithaca, New York 14850

In perfect and as well as in imperfect dielectric crystals, both the specific heat and thermal conductivity are basically well understood. In noncrystalline solids, however, recent experiments have resulted in several observations for which at this time no generally satisfactory explanation is available. In this lecture, we wish to summarize this work. We begin with a review of the properties of crystals. The sequence of the presentation will be as follows:

	crystals	glasses
specific heat	perfect: Figs. 1,2 imperfect: Figs. 3,4	Figs. 7 - 10
thermal conductivity	perfect: Fig. 5 imperfect: Fig. 6	Figs. 11-15

Specific Heat of Crystals

The specific heats of pure KCl, TiO_2, and graphite are shown in Fig. 1. The solid curves are computed, based on a three-dimensional Debye model. This model describes the KCl data very well, and the TiO_2 data reasonably well. The origin of the deviation is known to be the dispersion of the actual phonons in the crystals, resulting in departures from the assumptions underlying a perfect Debye solid. At temperatures above one percent of the Debye temperature θ, the specific heat of graphite varies as T^2. This has been understood through the two-dimensional, layer structure of this carbon allotrope.[2] Note that even this substance displays a lattice specific heat varying as T^3 at very low temperatures. The quality of the fit achieved using the Debye model is shown in Fig. 2, where the ratio of the measured specific heat to that calculated from the Debye model, using only the Debye-averaged sound velocities, has been plotted for four crystals. In all pure crystals studied to-date, the measured specific heat agrees with the Debye specific heat at temperatures below $10^{-2}\theta$ to within a few percent. It seems reasonable to conclude that dispersion has no influence on the plane wave excitations whose wavelengths are longer than 100 lattice spacings.

The density of states of the normal modes in pure crystals becomes small at low temperatures, and consequently small amounts of impurities can drastically alter the specific heat of crystalline solids. As an example, Fig. 3 shows the specific heat of KCl containing different concentrations of CN^-- ions substituting for Cl^-- ions. The excess specific heat is attributed to motional states of the CN^- ion tunneling between different equilibrium orientations (the six <100> directions in the cubic host). The anomaly associated with these tunneling states is of the Schottky type. At high concentrations, the anomaly is seen to broaden (Fig. 3, top curve). This is caused by inhomogeneous level broadening of the tunneling states resulting from the elastic dipole moments of the CN^-- ions.[4] Evidence for the influence of random internal stresses present even in pure or lightly doped crystals has been found in specific heat measurements on NaBr:F.[5] Here the small F^-- ion can tunnel between several equivalent equilibrium positions in the Br^-- vacancy. The tunnel splitting is small in this case, and hence even the small internal stresses can show up by lowering some potential minima, and raising others. What is seen in the specific heat is a manifestation of the energy required for the F^-- ion to jump from a lower to a higher minimum. The random stresses give rise to an almost linear specific heat anomaly, see Fig. 4.

Thermal Conductivity of Crystals

The thermal conductivity of pure dielectric crystals shows qualitatively the same behaviour for all materials, see Fig. 5. The conductivity rises with decreasing temperature, as the momentum destroying Umklapp collisions become less frequent. When their mean free path approaches that of the sample, the conductivity goes through a maximum, and then decreases with the specific heat. In this region, the conductivity $\varkappa(T) = \frac{1}{3} C\, v\ell \propto (1/3)\, \frac{T^3}{v^3}\, vd$, where T is the temperature, v the Debye averaged sound velocity, and d the sample diameter. C and ℓ are specific heat and average phonon mean free path respectively.

Impurities have a strong influence on the thermal conductivity of dielectric crystals. In the example shown in Fig. 6 the conductivity is greatly reduced by small concentrations of CN^-- ions dissolved in KCl. The resonant scattering causing the dips in the curves at 0.5 and 5°K results from phonon scattering by the quasi-rotational states of the CN^- ions.

Specific Heat of Glasses

In glasses, the phonon dispersion is different from that of crystals. Nevertheless, the specific heat of the glassy phase is little different from the crystalline phase, at least in the temperature region above 1°K (typically $10^{-2}\theta$). Fig. 7 shows an example. The peak in the ratio of experimental to Debye specific heat (see Fig. 2) moves to lower temperatures in the glassy phase. The only real surprise is that even at temperatures below $10^{-2}\theta$ the vitreous phase specific heat has <u>not</u> approached the Debye value as determined by the elastic properties of the glass. Measurements to lower temperatures, see Fig. 8, have in fact revealed an even stronger deviation. In the vicinity of 0.1K, the specific heat is dominated by a linear term. Fig. 9 demonstrates that this phenomenon is sample independent and also independent of the experimenter. In Fig. 10, the same data, together with data obtained on a large number of different noncrystalline solids, have been plotted as specific heat divided by temperature, C/T, versus T^2, on a doubly linear scale. The data lie on straight lines. Hence, the specific heat in this temperature range can be represented by a polynomial:

$$C = AT + BT^3.$$

At higher temperatures, the addition of a T^5-term improves the fit. As can be seen in Fig. 9 for the case of silica, the T^5-term marks the onset of the bump in the $C_{\text{experiment}}/C_{\text{Debye}}$ plot.

The occurrence of a linear term in the specific heat of electrical insulators, whose magnitude is practically independent of the host and also of the particular sample measured, is an extraordinary result. An additional surprise, as remarked above, is the fact that the BT^3 term used to describe the specific heat is considerably larger than the one computed from sound velocity measurements using the Debye model. We will summarize this later in a table. At this point, note that in Fig. 10 the influence of the BT^3 term is noticeable even at temperatures of the order of 0.2 K, i.e. typically $10^{-3}\theta$. Compare this with the rapid approach to the Debye value in the crystalline phase, as the temperature is lowered (see Fig. 7, and also Fig. 2).

Thermal Conductivity of Glasses

The thermal conductivity of noncrystalline solids is known to be much smaller than that of crystals. Fig. 11 shows this for the two phases of SiO_2. Obviously, the disorder severely limits the heat transfer. It is, nevertheless, interesting to note that a highly doped crystal may have a thermal conductivity even lower than silica, see Fig. 11 (pure KCl has a conductivity accidentally almost equal to that of crystal quartz).

SiO_2 can be mixed with many oxides, thus forming the large family of silica based glasses, whose structure is schematically represented in Fig. 12. None of these glasses have a conductivity different from that of pure silica, see Fig. 13. Even the inevitable accidental impurities like water, hydroxyl, or iron, known to severely alter the conductivity of crystalline solids, do not seem to affect the conductivity. Obviously again, the intrinsic low conductivity of silica is expected to be less sensitive to impurities and to an increase in the disorder, but the fact remains that a phonon scattering center equivalent to the CN^- ion in KCl (Fig. 11) has not been found yet, even though a large number of glasses has been measured.

In Fig. 14 we show a plot of the low temperature thermal conductivities of several noncrystalline solids. Not only do all curves have similar shapes, but they also have similar magnitudes. Moreover, below 1°K, the conductivities are described by a power law: $\varkappa(T) = a(T/°K)^d$, where d is very nearly the same for all glasses.

Summary

We summarize the findings on specific heat and thermal conductivity of glasses in Table I. The second column lists A, the coefficient of the linear specific heat term. For comparison, the magnitude of the linear specific heat term in copper is $\gamma = 12 \cdot 10^{-6}$ Watt second $gram^{-1}$ K^{-2}. In column 3 and 4, we compare the measured T^3 term with that predicted from the Debye model, $B_{el}T^3$. On the average, $B \sim 2B_{el}$. Finally, the power d of the temperature dependence of the thermal conductivity, is d = 1.8, with an absolute error estimated to be 0.1, and with little variation from substance to substance, as shown in the Table.

The only exceptions from this general behaviour are shown in Fig. 15: The partially crystallizing solids nylon, teflon, and polyethylene have thermal conductivities which depend on the material as well as on the sample, and their conductivities are up to one order of magnitude smaller than those of the fully noncrystalline polymers polystyrene and polymethyl methacrylate, or of vitreous silica. Apparently, what no impurity, and no increase in the disorder can achieve, can be achieved by letting part of the glass crystallize!

Theoretical Models

We wish to mention briefly the explanations which have been proposed for the anomalous behaviour of glasses. For details, we refer to the original papers.

A spread of low-lying electronic[6] states has been suggested, possibly connected with the bound states in the gap of amorphous semiconductors. The absence of a magnetic field dependence of both the specific heat (reviewed by Zeller and Pohl, ref. 1) and thermal conductivity[7] as well as the absence of a magnetic susceptibility of undoped amorphous semiconductors,[8] however, impose rather stringent restrictions on the nature of such states.

An effective random internal stress associated with the disorder in glasses could possibly produce several potential minima between which certain atoms in the glassy structure could tunnel. The picture is similar to the one adopted for NaBr:F which was based on the earlier work by Sussmann.[9] This atomic tunneling model has been discussed in quantitative detail,[10] and the conditions for the distribution of tunneling rates and for the coupling to the phonons have been derived.

A distribution of voids of different diameters in amorphous materials has been postulated, in which trapped atoms have low lying energy states approximated by the states of a particle in a square well potential.[11] Independent evidence for such voids has not been reported though, and neither has the problem of the phonon scattering by these defects been considered.

The phonon dispersion curve, $\omega(k)$, of a crystal, approaches zero not only near the center of the zone, but also at $k = 2\pi/a$, where a is the interatomic spacing. In polycrystalline materials, glasses, and liquids, this second minimum is washed out but in liquid helium it is well defined and gives rise to the dip in the dispersion curve known as the roton minimum. It has been proposed that in glasses, a similar "roton-like" minimum exists and comes close enough to the $\omega = 0$ axis so that in conjunction with its spread, it may cause the linear specific anomaly.[12]

Finally, it has been suggested that the long wavelength, $k \approx 0$, elastic excitations are strongly damped because of visco-elastic effects.[13] The assumption is that as the stress wave propagates through the glass, the glassy structure relaxes to a different equilibrium position. This effect is suggested to explain both the thermal conductivity and the specific heat. At present, no independent experimental evidence has been reported for the relaxation process which takes place with the required short time of approximately 10^{-13} sec at low temperatures.

Although arguments in favor of all the models mentioned above can be made, it is not clear whether any of them can pass the most important test, namely that whether they are sufficiently general to account for as general a phenomenon as has been observed in such a wide variety of glasses. In particular, any models considering processes occurring on the atomic scale should be scrutinized carefully from this viewpoint.

Regardless of which model finally turns out to be correct, however, we know one thing with certainty: Once we understand the observations summarized here, we will have enhanced our understanding of the amorphous state to a significant degree.

References

* Supported by the U. S. Atomic Energy Commission, under Contract AT(11-1)-3151, Technical Report #COO-3151-13.

1. Much of the work reviewed here has been reported by R. C. Zeller and R. O. Pohl, Phys. Rev. B 4, 2029 (1971) and by R. B. Stephens, G. S. Cieloszyk and G. L. Salinger, Phys. Letters 38A, 215 (1972). For the sake of brevity we will give references in this paper only to work that has not been mentioned in these two papers.
2. J. A. Krumhansl and H. Brooks, J. Chem. Phys. 21, 1663 (1952).
3. Reviewed in V. Narayanamurti and R. O. Pohl, Rev. Mod. Physics 42, 201 (1970).
4. J. P. Harrison, P. P. Peressini, and R. O. Pohl, Phys. Rev. 182, 939 (1966).
5. R. J. Rollefson, Phys. Rev. B 5, 3235 (1972).
6. D. Redfield, Phys. Rev. Letters 27, 730 (1971); T. A. Kaplan, S. D. Mahanti, and W. M. Hartmann, Phys. Rev. Letters 27, 1796 (1971).
7. L. J. Challis and C. N. Hooker, J. Phys. Chem. Solids 5, 1153 (1972).

8. D. U. Gubser and P. C. Taylor, Phys. Letters 40 A, 3 (1972), B. G. Bagley, F. J. DiSalvo, and J. V. Waszczak, Solid State Comm. 11, 89 (1972).

9. J. A. Sussmann, Physik Kondensierten Materie 2, 146 (1964), and R. Pirc, B. Zeks, and P. Gosar, J. Phys. Chem. Solids 27, 1219 (1966).

10. P. W. Anderson, B. I. Halperin, and C. M. Varma, Phil. Mag. 25, 1 (1972), and W. A. Phillips, J. Low Temp. Phys. 7, 351 (1972).

11. H. Rosenstock, J. Noncryst. Solids 7, 123 (1972).

12. S. Takeno, see the Proceedings of this conference.

13. P. Fulde and H. Wagner, Phys. Rev. Letters 27, 1280 (1971).

Table I

Summary of data available on low temperature specific heat and thermal conductivity of noncrystalline solids. The data on Lexan are a private communication from G. S. Cieloszyk and G. L. Salinger.

MATERIAL	$C = AT + BT^3$		$C = B_{el.} T^3$	$\varkappa = a(T/K)^d$	
	A $\frac{10^{-6} ws}{g\,K^2}$	B $\frac{10^{-6} ws}{g\,K^4}$	$B_{el.}$ $\frac{10^{-6} ws}{gK^4}$	a $\frac{10^{-4} w/cm\ K}{}$	d
SiO_2	0.97	2.1	.81	2.2	1.74
$Na_2O\ (SiO_2)_3$	2.0	2.5	1.12		
Pyrex	~1	2.2	1.13	1.9	1.75
GeO_2	0.75	2.7	1.95	3.6	1.87
As_2S_3	1.4	13.8	7.85	13.	1.83
B_2O_3	1.25	10.5	7.8	2.8	1.85
BeF_2		4.4	2.22		
Se	0.8	21.	17.0	9.1	1.87
PMMA	4.4	33.	18.2	2.8	1.76
PS	5.2	46.	25.5	1.6	1.78
$K\ Ca(NO_3)_3$	5.7	19.4	16.6	1.4	1.83
Glycerol	~2	11.			
GE 7031				4.3	1.76
Lexan	3.8	41.	28.5	2.	

Figure Captions

Figure 1. Reduced specific heat for three different crystals, compared with the Debye theory based on elastic measurements (solid lines). R = Gas Constant = 8.31 Watt sec mole^{-1} K^{-1}, mole = (A) gram, with (A) being the average atomic weight of the host atoms. θ = Debye temperature. References: KCl: P. H. Keesom and N. Pearlman, Phys. Rev. 91, 1354 (1953); W. T. Berg and J. A. Morrison, Proc. Roy. Soc. (London) 242, 467 (1957). TiO_2: T. R. Sandin and P. H. Keesom, Phys. Rev. 177, 1370 (1969). J. S. Dugdale, J. A. Morrison, and D. Patterson, Proc. Roy. Soc. (London) A 224, 228 (1954). Graphite: W. De Sorbo and W. W. Tyler, J. Chem. Phys. 21, 1660 (1953); W. De Sorbo and G. E. Nichols, J. Phys. Chem. Solids 6, 352 (1958), B. J. C. Van der Hoeven and P. H. Keesom, Phys. Rev. 130, 1318 (1963).

Figure 2. Deviation of the experimental specific heat $C_{v,exp}$ from the Debye prediction, plotted as $C_{v,exp}/C_{v,\text{ Debye}}$. References: KCl and TiO_2, see Fig. 1; Se: see Ref. 1. Ge: P. H. Keesom and N. Pearlman, Phys. Rev. 91, 1347 (1953); R. W. Hill and D. H. Parkinson, Phil. Mag. (7) 43, 309 (1952).

Figure 3. Specific heat of KCl and KCl:CN for various concentrations. Ref. 4 and J. P. Harrison, private communication. The dashed lines are Schottky anomalies computed for tunnel splittings

and CN^--concentrations determined by independent methods, see ref. 3.

Figure 4. Specific heat of NaBr:F, ref. 5.

Figure 5. Thermal conductivity of pure dielectric crystals. References: He^4, D. T. Lawson, Ph. D. Thesis, Duke University, 1972, unpublished; CsI, T. F. McNelly, Cornell, private communication; LiF, P. D. Thacher, Phys. Rev. 156, 975 (1967); α-quartz, R. C. Zeller and R. O. Pohl, ref. 1. Argon, G. K. White and S. B. Woods, Phil. Mag. 3, 785 (1958). In this argon crystal, the thermal conductivity in the boundary scattering region is limited by grain boundaries. In a single crystal, it would be higher than that of CsI.

Figure 6. Thermal conductivity of KCl:CN. After W. D. Seward and V. Narayanamurti, Phys. Rev. 148, 463 (1966), and ref. 3.

Figure 7. Specific heat of vitreous and of crystalline SiO_2 above 2 K.

Figure 8. Specific heat of the two phases of SiO_2 above 0.1K, ref. 1.

Figure 9. Comparison of the specific heat of five samples of vitreous silica measured by different experimenters (see ref. 1).

Plotted is the measured specific heat divided by T^3.

Figure 10. Specific heat of several noncrystalline solids, plotted as C_v/T vs. T^2. Ref. 1. The intercept with the vertical axis determines the linear specific heat term, the slope of the straight lines determines the T^3 term. PS: polystyrene, PMMA: polymethylmethacrylate (plexiglass).

Figure 11. Thermal conductivity of vitreous and crystalline SiO_2, and of KCl:CN (bottom curve of Fig. 6). Ref. 1.

Figure 12. Two-dimensional, schematic, representation of the lattices of quartz (a), silica (b), and of silica based glasses (c). After Zachariasen and Warren, see B. E. Warren, J. Am. Ceram. Soc., 24, 256 (1941).

Figure 13. Thermal conductivity of vitreous silica and silica-based glasses, like borosilicates, Crown glass, soda-lime glasses. See Zeller and Pohl, ref. 1.

Figure 14. Thermal conductivity of noncrystalline solids. Ref. 1. The data on As_2S_3 above 1 K after A. Leadbetter, private communication.

Figure 15. Thermal conductivity of partially (~ 50%) crystallized glasses. Curves B, D, and G after W. Reese and J. E. Tucker, J. Chem. Phys. 43, 105 (1965); C and F after A. C. Anderson,

W. Reese, and J. C. Wheatley, Rev. Sci. Instr. 34, 1386 (1963); E after R. Berman, Proc. Roy Soc. (London) A 208, 90 (1951); H after R. L. Powell, W. M. Rogers, and D. O. Coffin, J. Res. Natl. Bur. Standards 59, 349 (1957); I and J, G. L. Salinger, in Amorphous Materials, R. W. Douglas and B. Ellis, ed., Wiley-Interscience, New York 1972, p. 475.

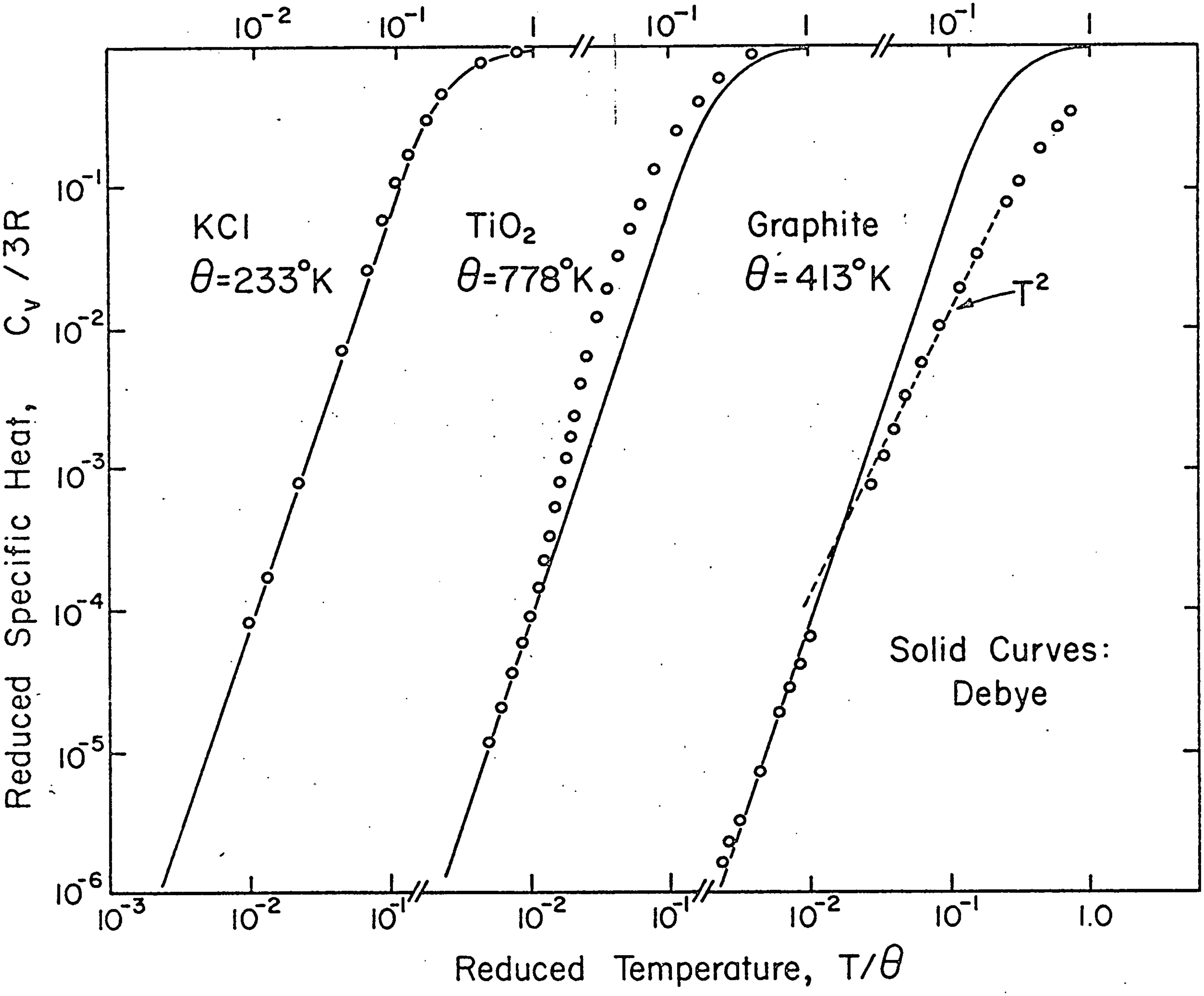
10^-2
10^-1
1
10^-1
1
10^-1
1
KCl
θ=233°K
TiO₂
θ=778°K
Graphite
θ=413°K
T²
Solid Curves:
Debye
Reduced Specific Heat, Cv /3R
10^-1
10^-2
10^-3
10^-4
10^-5
10^-6
10^-3
10^-2
10^-1
10^-2
10^-1
10^-2
10^-1
1.0
Reduced Temperature, T/θ

Figure 1

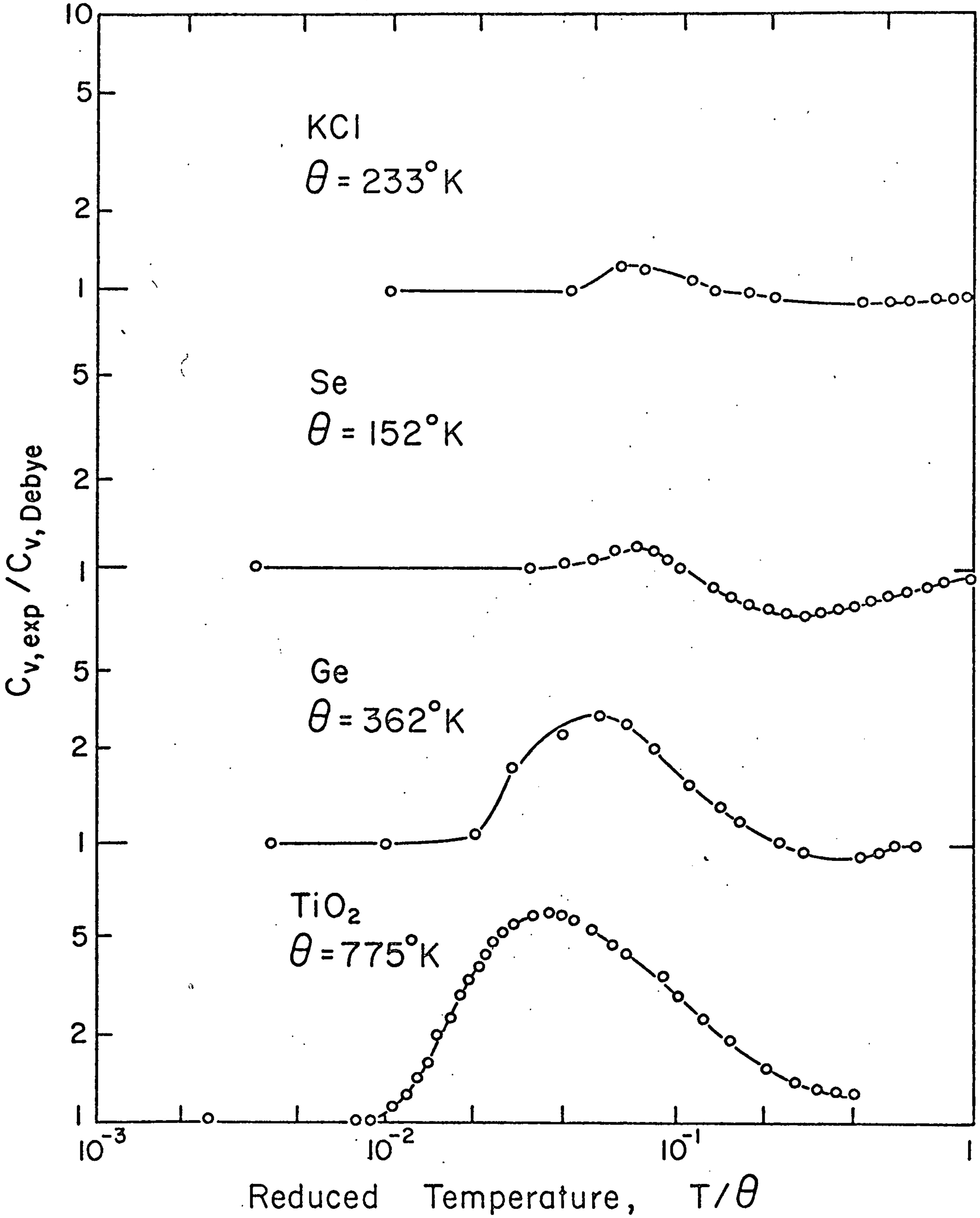

10
5
2
1
5
2
1
5
2
1
5
2
1
KCl
$\theta = 233°K$
Se
$\theta = 152°K$
Ge
$\theta = 362°K$
TiO_2
$\theta = 775°K$
$C_{v,exp} / C_{v,Debye}$
10^{-3}
10^{-2}
10^{-1}
1
Reduced Temperature, T/θ

Figure 2

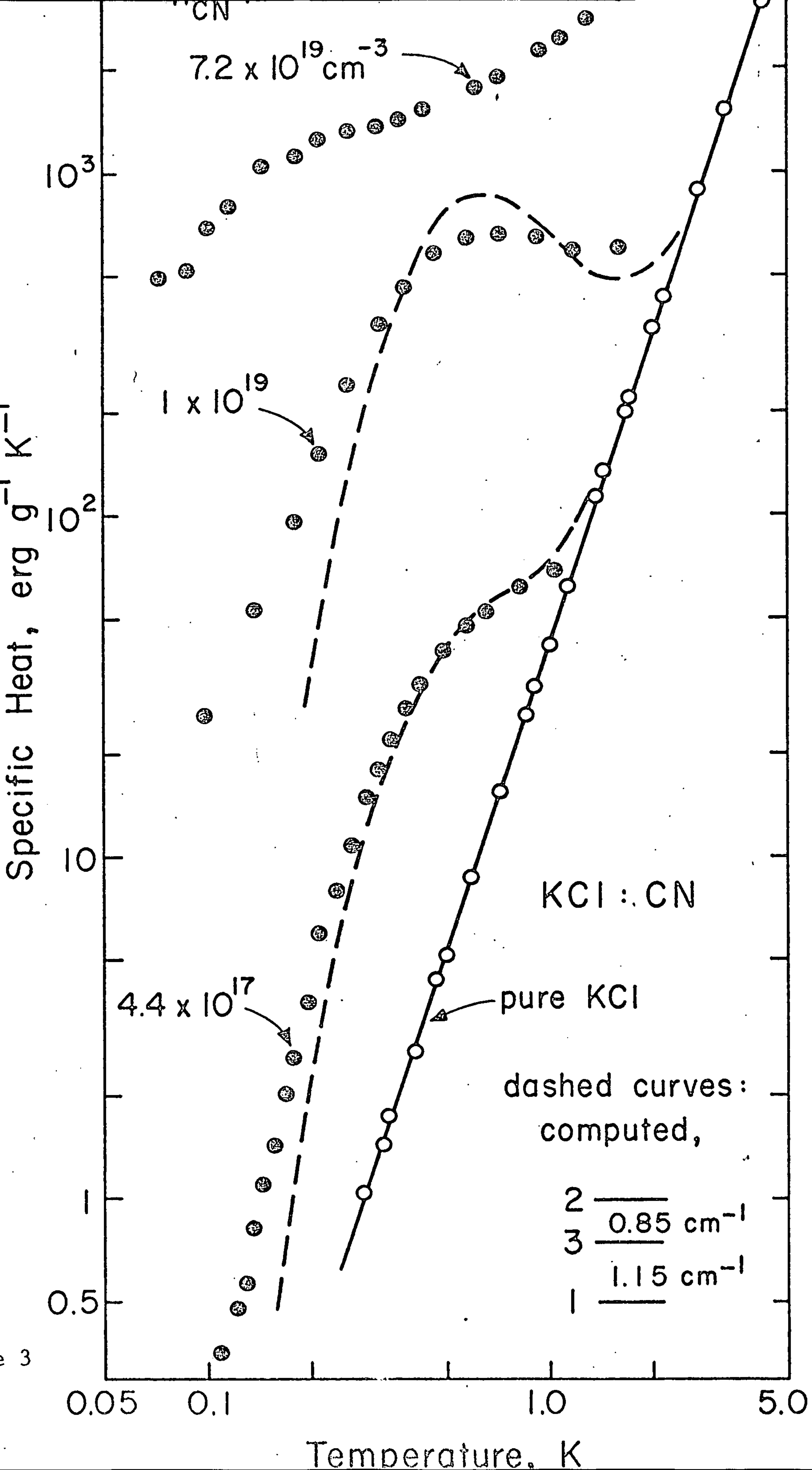

CN
7.2 x 10^19 cm^-3
1 x 10^19
4.4 x 10^17
pure KCl
KCl :. CN
dashed curves: computed,
2
0.85 cm^-1
3
1.15 cm^-1
1
Specific Heat, erg g^-1 K^-1
10^3
10^2
10
1
0.5
0.05
0.1
1.0
5.0
Temperature, K

Figure 3

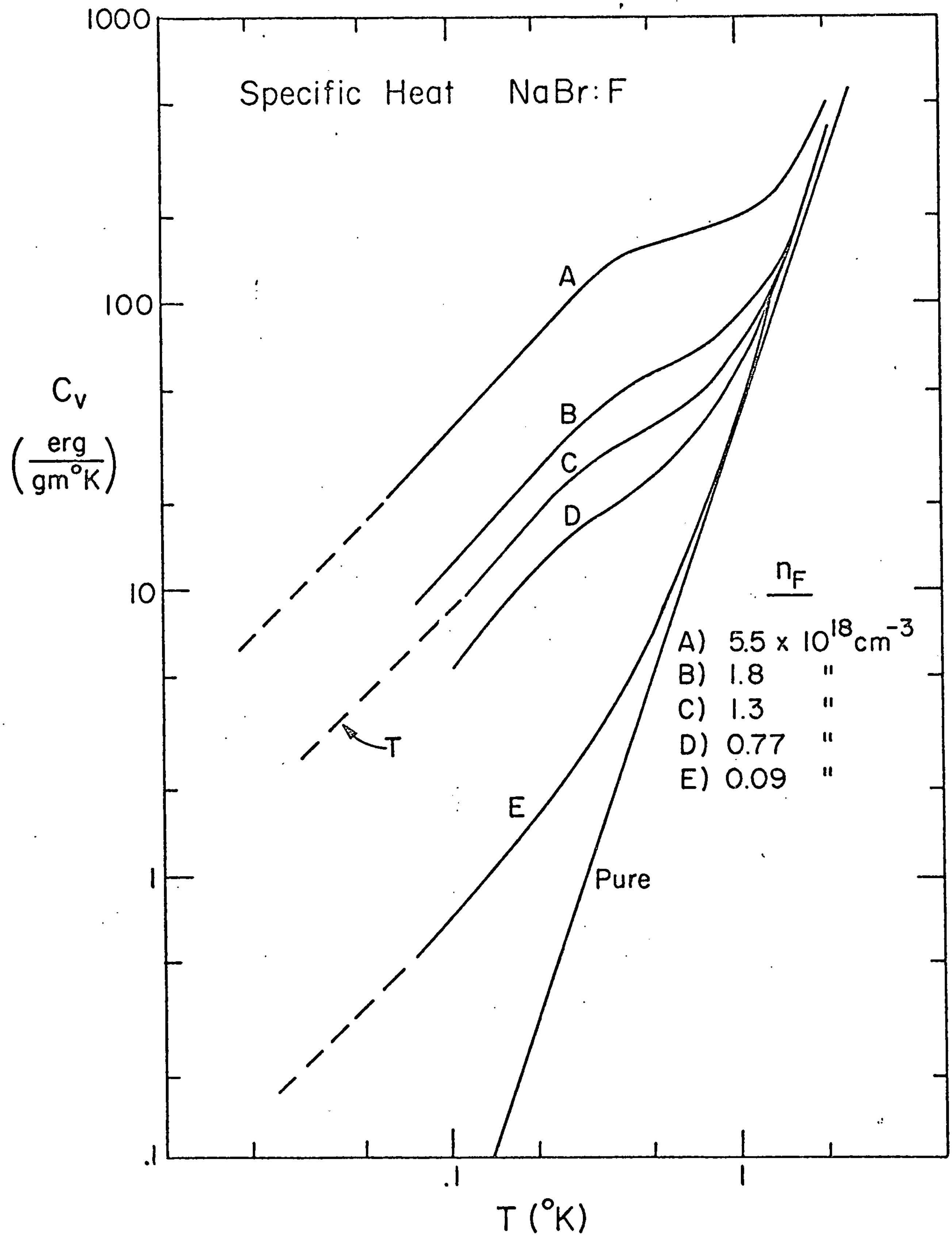

Specific Heat NaBr:F
1000
100
10
1
.1
C_v
$\left(\frac{erg}{gm^\circ K}\right)$
A
B
C
D
E
T
Pure
n_F
A) 5.5 x $10^{18}cm^{-3}$
B) 1.8 "
C) 1.3 "
D) 0.77 "
E) 0.09 "
.1
1
T (°K)

Figure 4

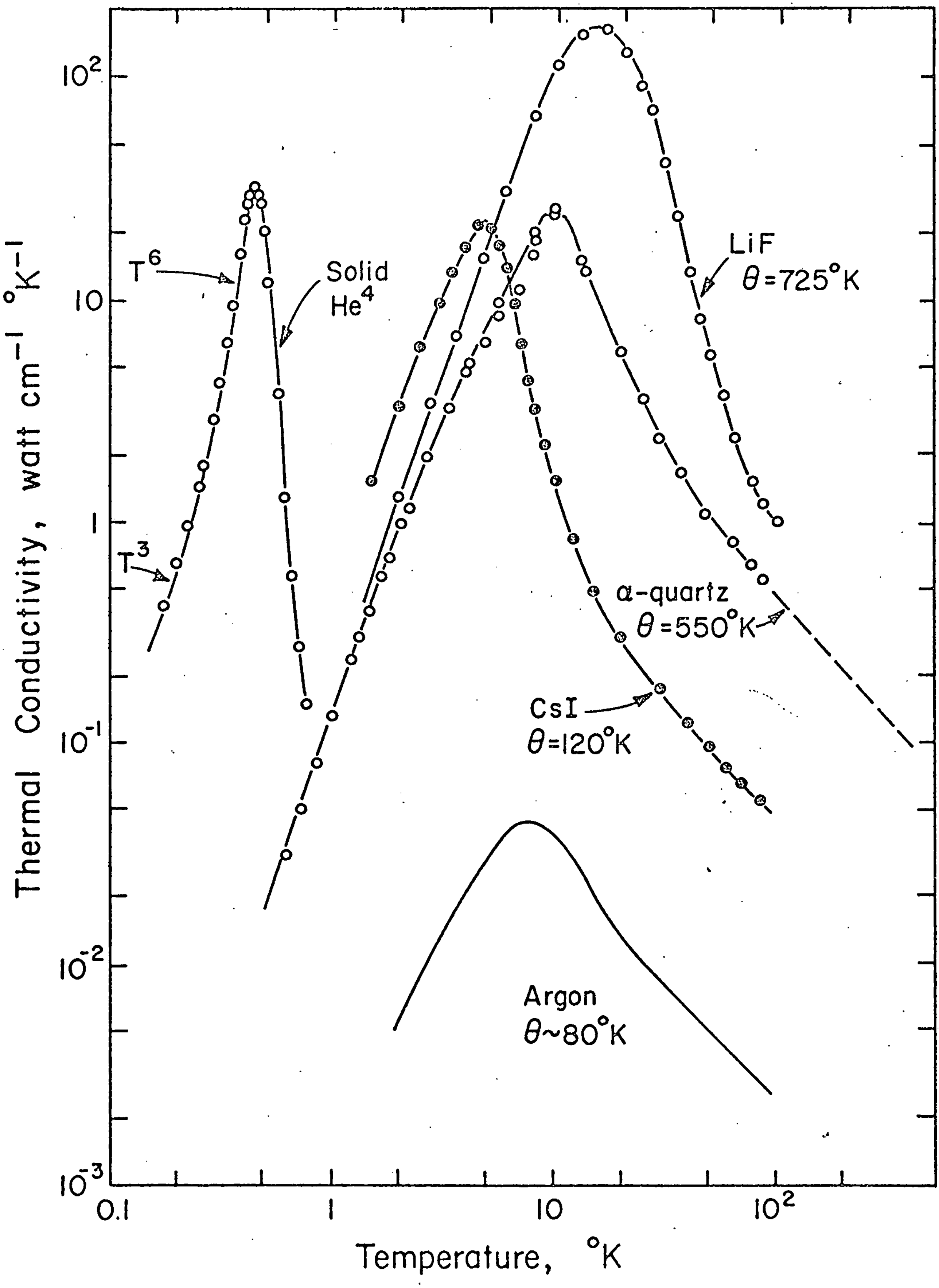

Thermal Conductivity, watt cm^{-1} °K^{-1}
Temperature, °K
10^2
10
1
10^{-1}
10^{-2}
10^{-3}
0.1
1
10
10^2
T^6
T^3
Solid He^4
LiF
θ=725°K
α-quartz
θ=550°K
CsI
θ=120°K
Argon
θ~80°K

Figure 5

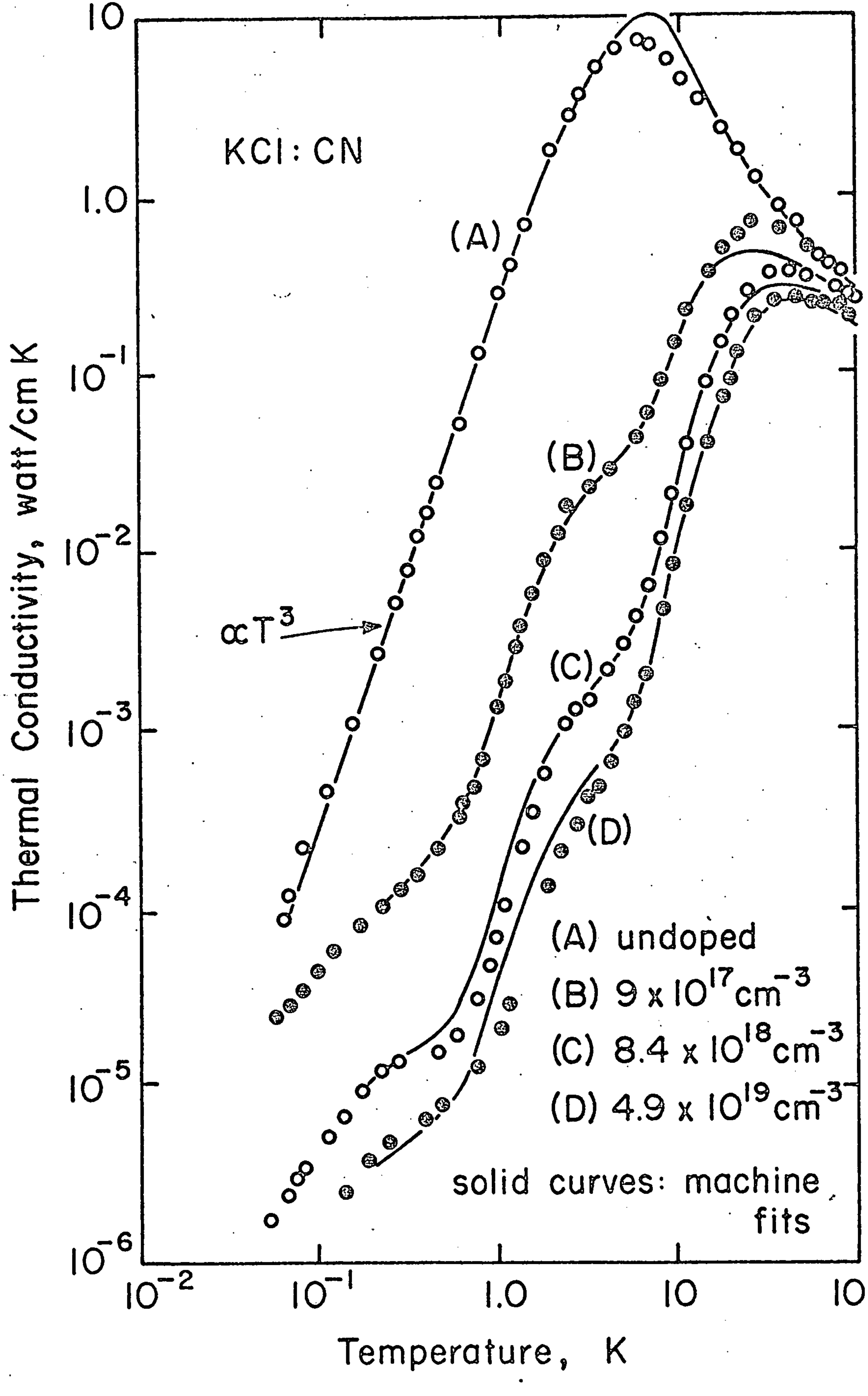
KCl : CN
(A)
(B)
(C)
(D)
∝T³
(A) undoped
(B) 9 x 10¹⁷cm⁻³
(C) 8.4 x 10¹⁸cm⁻³
(D) 4.9 x 10¹⁹cm⁻³
solid curves: machine fits
Thermal Conductivity, watt/cm K
10
1.0
10⁻¹
10⁻²
10⁻³
10⁻⁴
10⁻⁵
10⁻⁶
10⁻²
10⁻¹
1.0
10
10²
Temperature, K

Figure 6

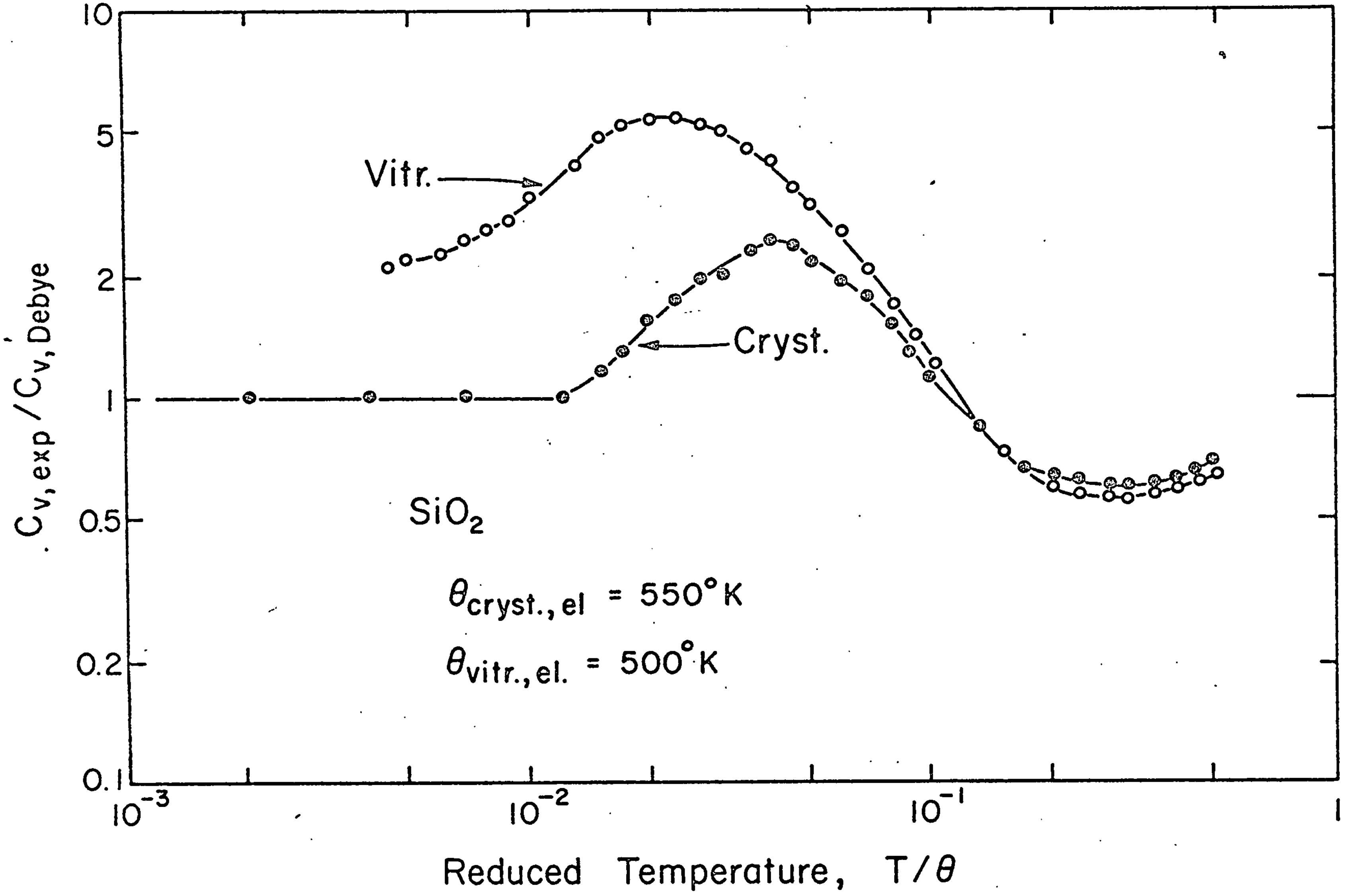

10
5
2
1
0.5
0.2
0.1
$C_{v,exp}/C_{v,Debye}$
Vitr.
Cryst.
SiO_2
$\theta_{cryst.,el} = 550°K$
$\theta_{vitr.,el.} = 500°K$
10^{-3}
10^{-2}
10^{-1}
1
Reduced Temperature, T/θ

Figure 7

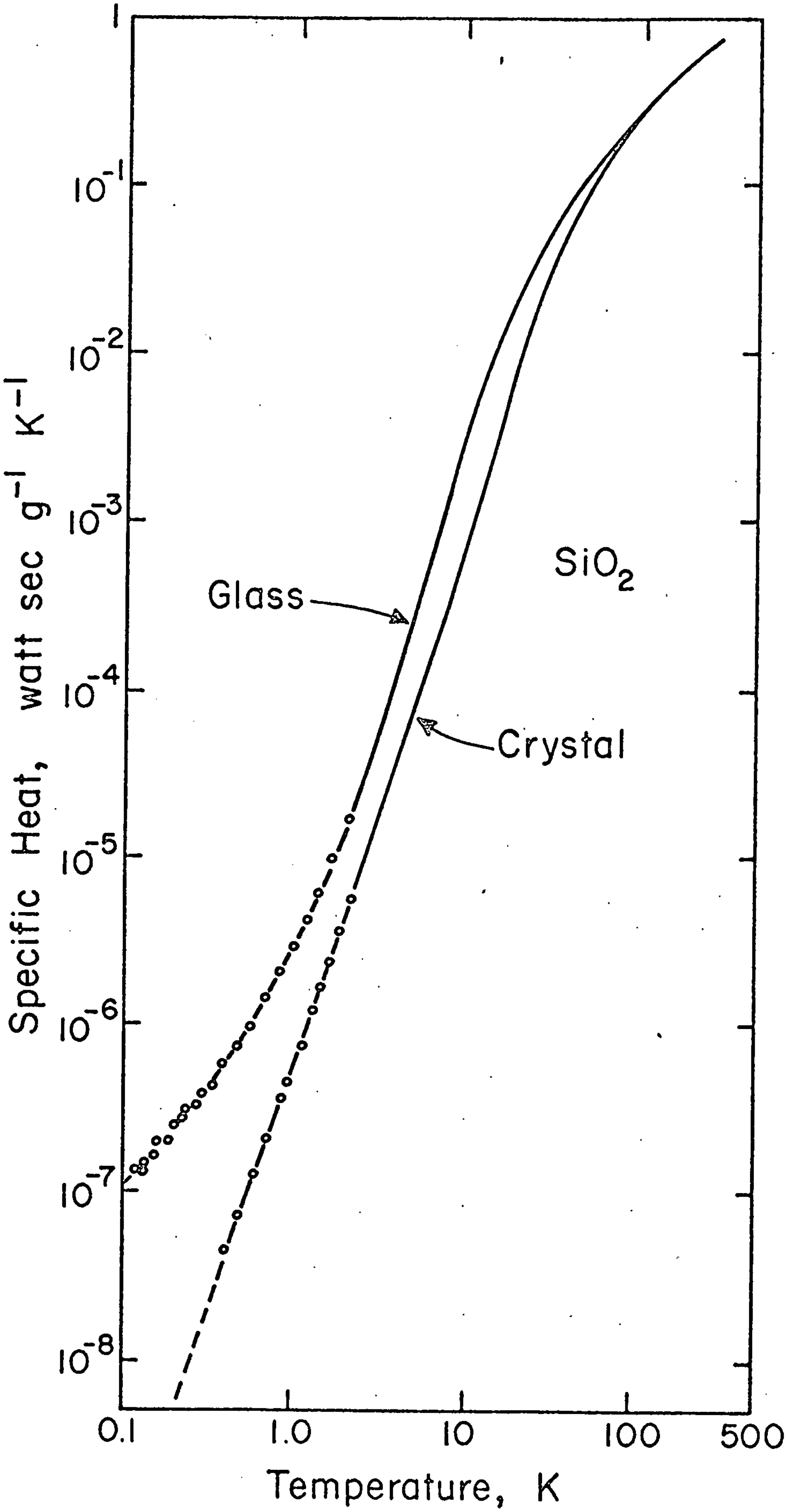

1
10^-1
10^-2
10^-3
10^-4
10^-5
10^-6
10^-7
10^-8
Specific Heat, watt sec g^-1 K^-1
SiO2
Glass
Crystal
0.1
1.0
10
100
500
Temperature, K

Figure 8

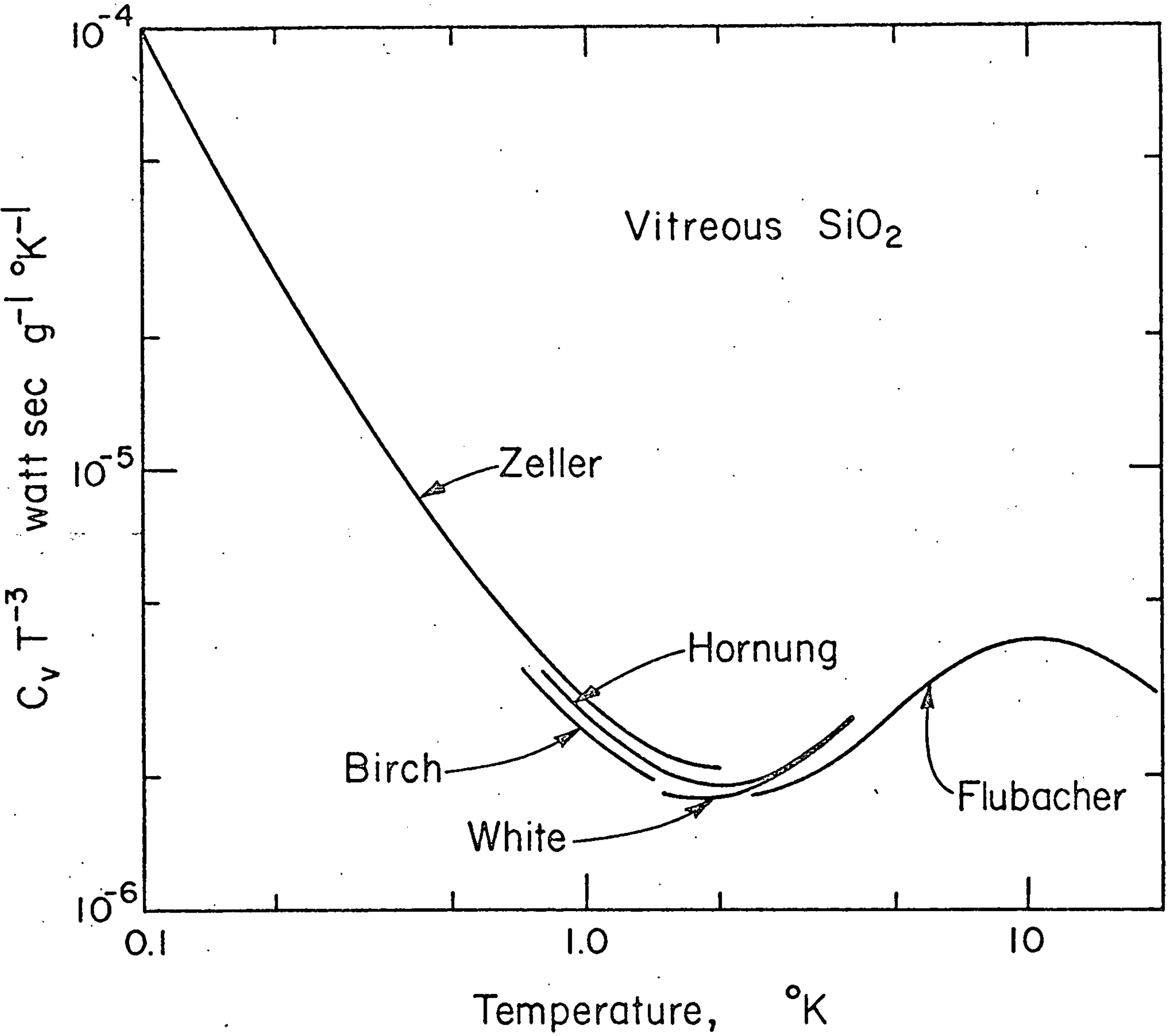

Vitreous SiO_2
$C_v T^{-3}$ watt sec g^{-1} °K^{-1}
10^{-4}
10^{-5}
10^{-6}
0.1
1.0
10
Temperature, °K
Zeller
Hornung
Birch
White
Flubacher

Figure 9

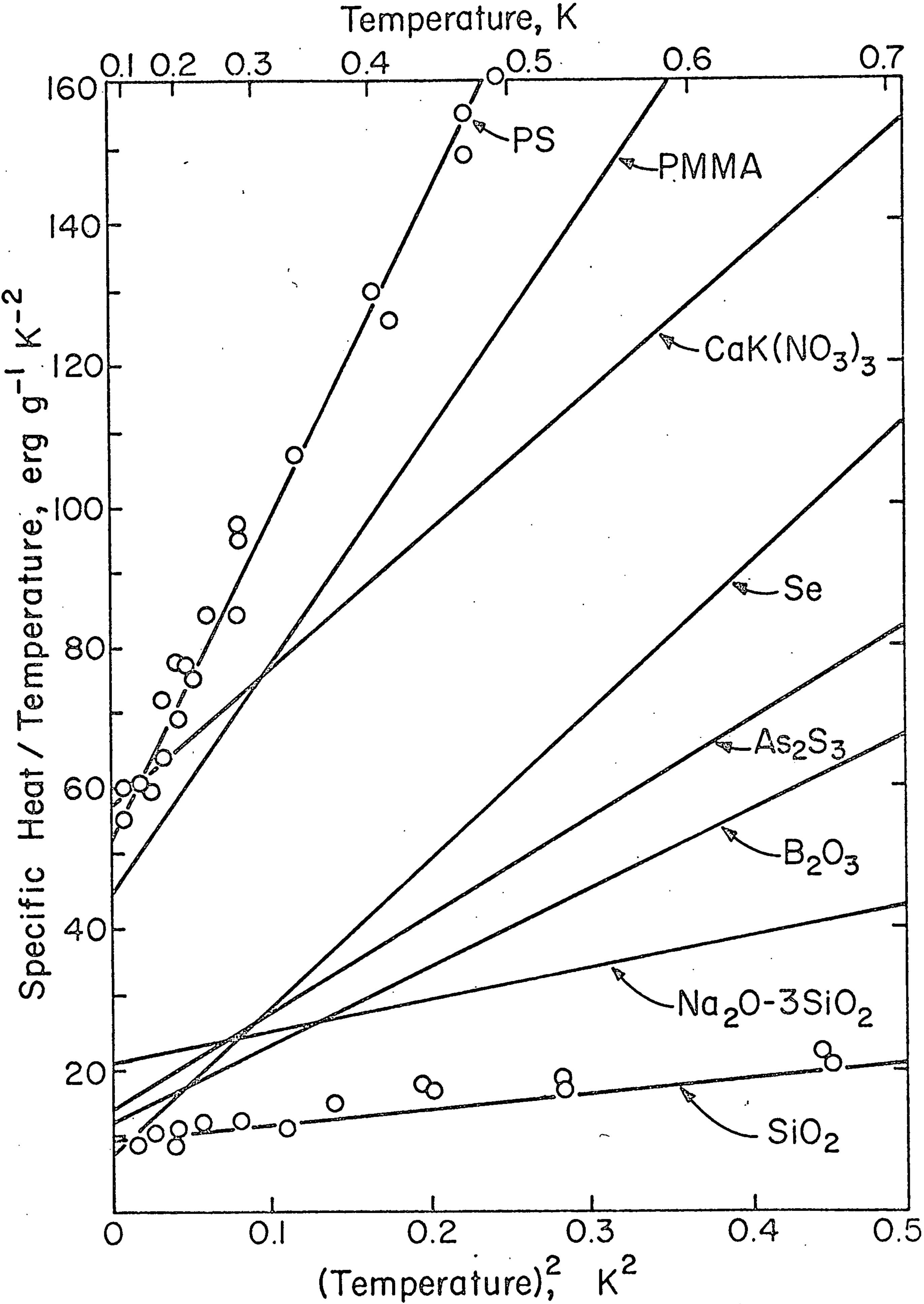
Temperature, K
0.1
0.2
0.3
0.4
0.5
0.6
0.7
160
140
120
100
80
60
40
20
0
0.1
0.2
0.3
0.4
0.5
Specific Heat / Temperature, erg g^{-1} K^{-2}
(Temperature)^2, K^2
PS
PMMA
CaK(NO$_3$)$_3$
Se
As$_2$S$_3$
B$_2$O$_3$
Na$_2$O-3SiO$_2$
SiO$_2$

Figure 10

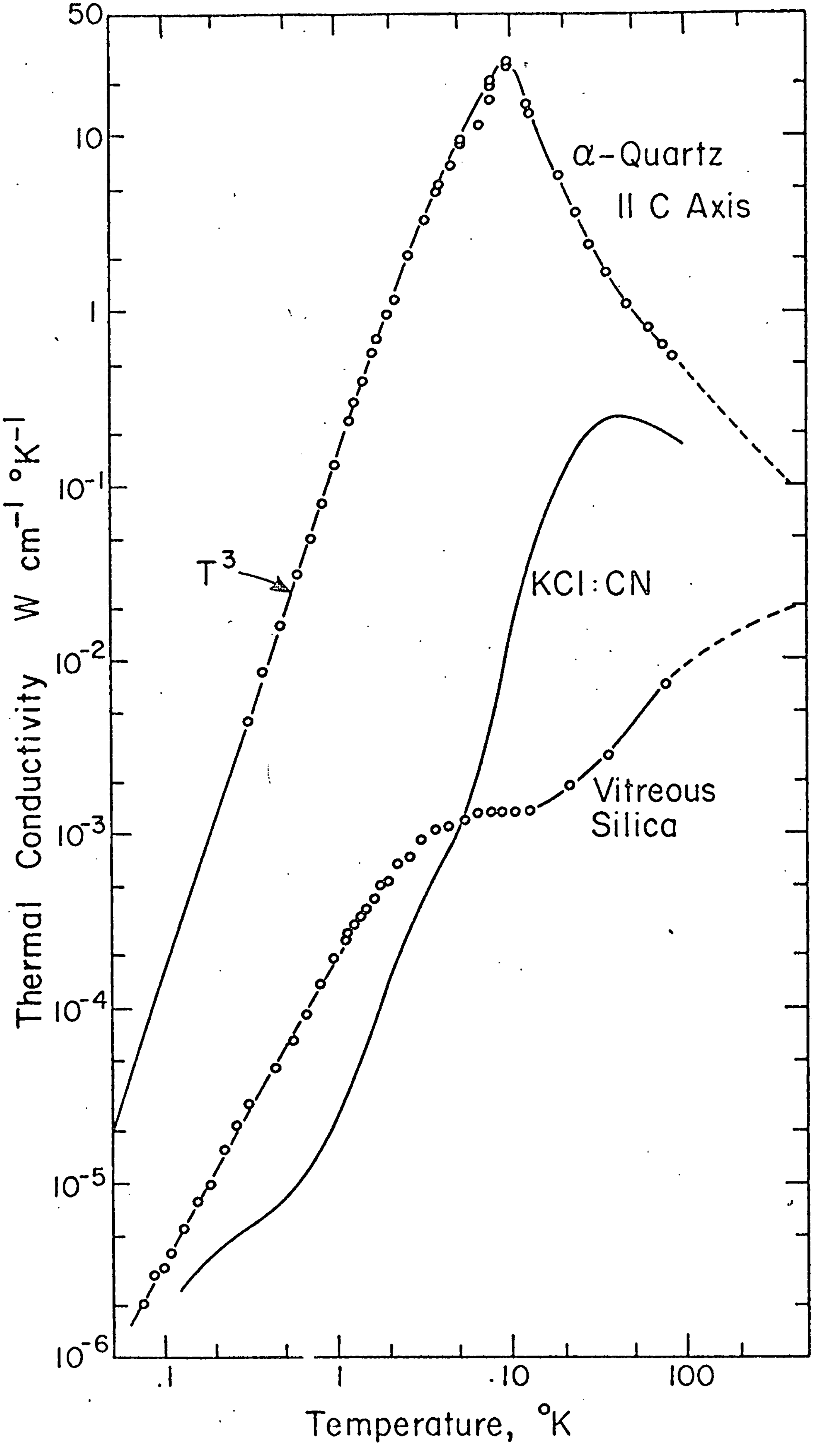

50
10
1
10^{-1}
10^{-2}
10^{-3}
10^{-4}
10^{-5}
10^{-6}
Thermal Conductivity W cm^{-1} °K^{-1}
.1
1
10
100
Temperature, °K
α-Quartz
‖ C Axis
T^3
KCl:CN
Vitreous
Silica

Figure 11

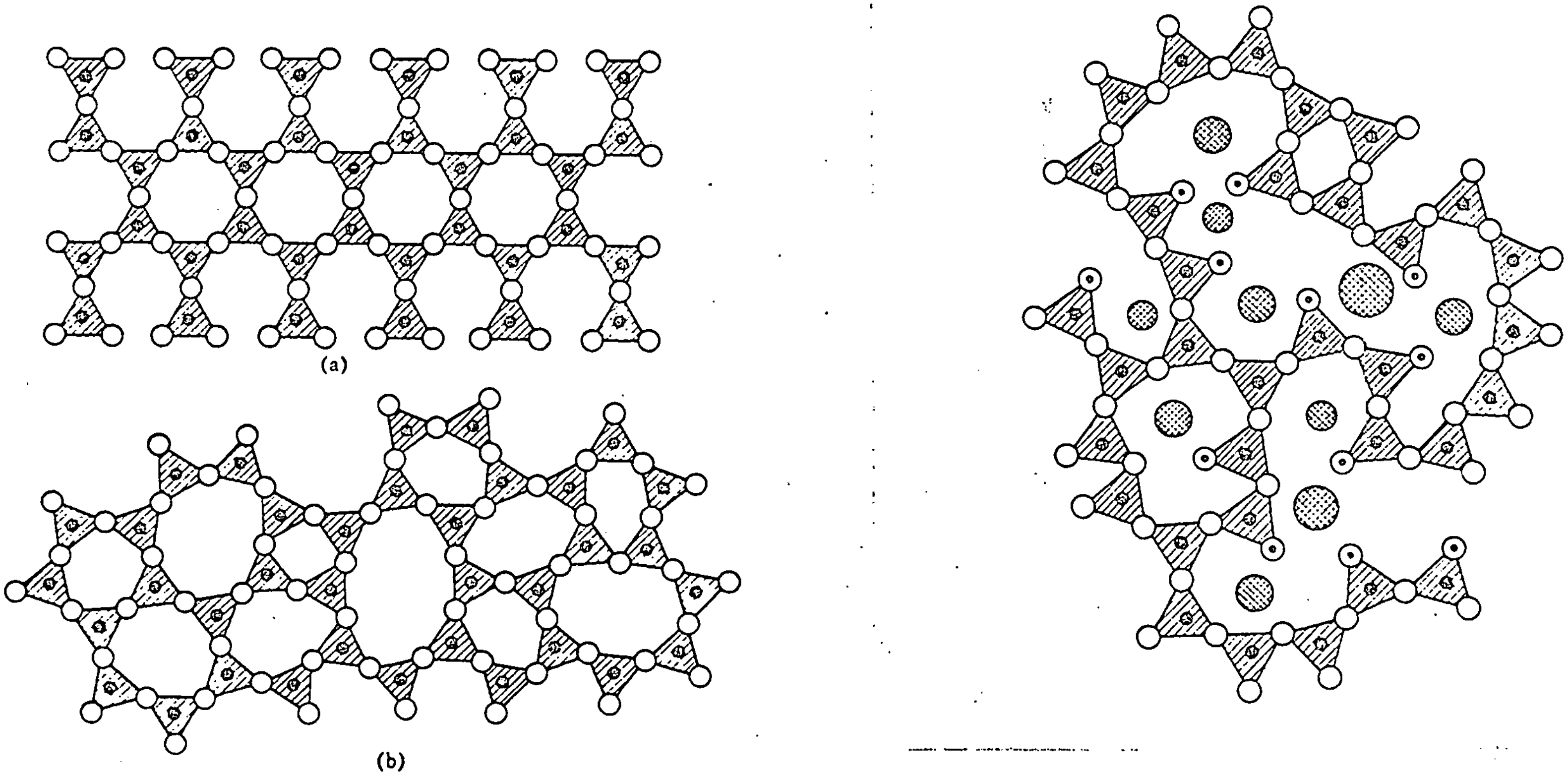
(a)

(b)

● Network former

○ Oxygen

● Network former

▨ Network modifier

○ Bridging oxygen

⊙ Non-bridging oxygen

Figure 12

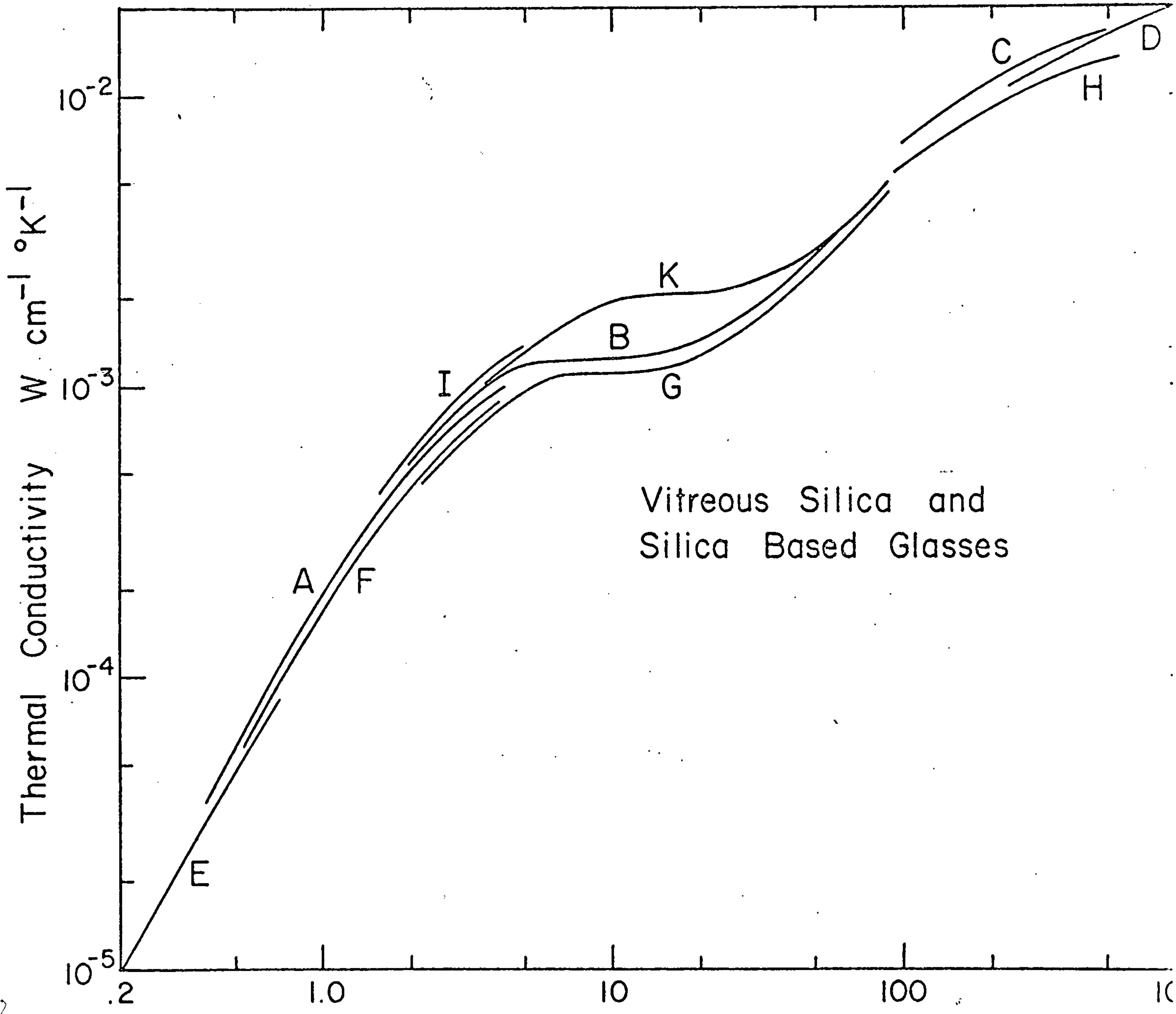
Thermal Conductivity W cm^{-1} °K^{-1}
10^{-2}
10^{-3}
10^{-4}
10^{-5}
.2
1.0
10
100
Temperature, °K
A
B
C
D
E
F
G
H
I
K
Vitreous Silica and Silica Based Glasses

Figure 13

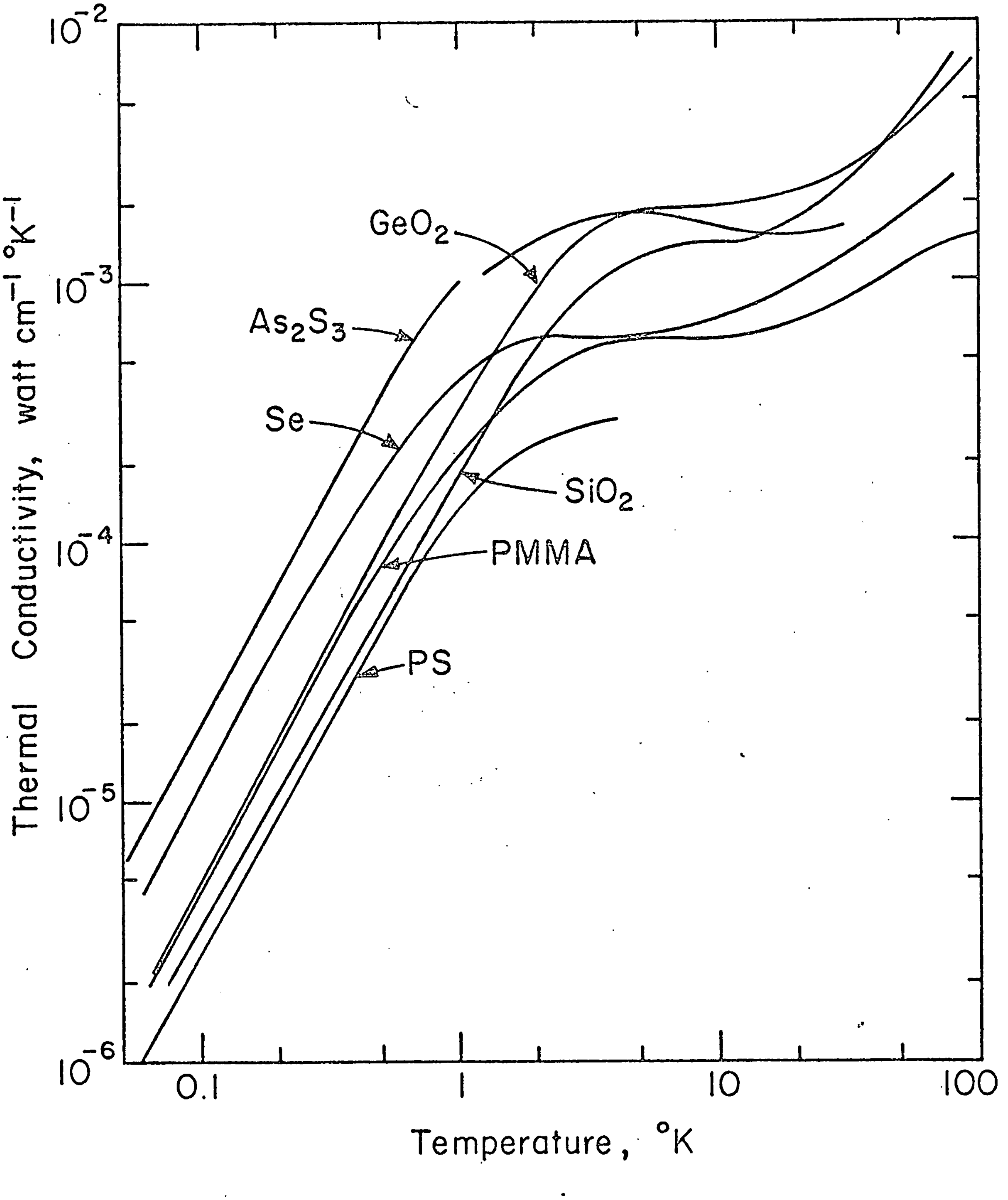

10^{-2}
10^{-3}
10^{-4}
10^{-5}
10^{-6}
Thermal Conductivity, watt cm^{-1} °K^{-1}
GeO_2
As_2S_3
Se
SiO_2
PMMA
PS
0.1
1
10
100
Temperature, °K

Figure 14

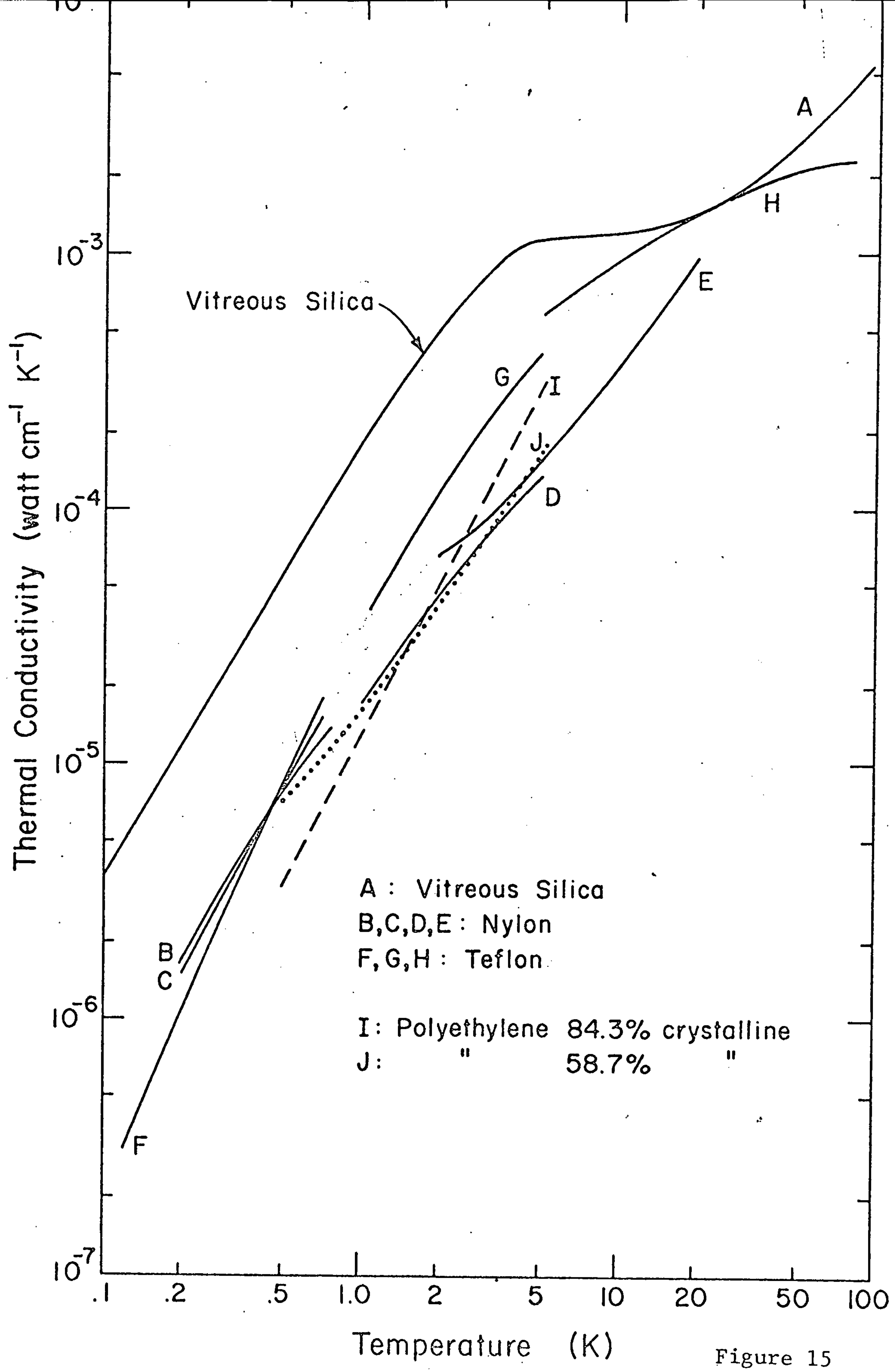

10
10^-3
10^-4
10^-5
10^-6
10^-7
Thermal Conductivity (watt cm^-1 K^-1)
.1
.2
.5
1.0
2
5
10
20
50
100
Temperature (K)
Vitreous Silica
A
H
E
G
I
J
D
B
C
F
A : Vitreous Silica
B,C,D,E : Nylon
F,G,H : Teflon
I: Polyethylene 84.3% crystalline
J: " 58.7% "

Figure 15